Molecular Structure and Crystal Organization of Neutral and Ionic Derivatives of $[M_4(CO)_{12}]$ (M = Co, Rh or Ir) Clusters and a Bonding Study by Extended-Hückel Calculations†

Dario Braga,*[a] Fabrizia Grepioni,[a] Janice J. Byrne[a] and Maria José Calhorda*[b]
[a] *Dipartimento di Chimica G. Ciamician, Università di Bologna, Via Selmi 2, 40126 Bologna, Italy*
[b] *Instituto de Tecnologia Química e Biológica, R. da Quinta Grande 6, 2780 Oeiras, and Instituto Superior Técnico, Lisboa, Portugal*

The molecular and crystal structures of neutral and ionic derivatives of $[M_4(CO)_{12}]$ (M = Co, Rh or Ir) clusters have been studied by a combined use of molecular-orbital calculations of the extended-Hückel type and packing analysis. The problem of the existence of two structural forms, namely the 'all-terminal' structure with no bridging carbonyl ligands and the 'bridged' structure with three edge-bridging carbonyls, in the solid state has been addressed. The presence of intermolecular hydrogen-bonding interactions of the C–H···O type between carbonyl groups and the hydrogen atoms of the cations has been investigated.

In previous studies we have shown that much can be learned on the relationship between the structure of a given molecule and that of its crystal by investigating *simultaneously* the two systems with adequate techniques.[1] The molecular and crystal structures are interdependent, *viz.* the structural properties of an individual molecular entity influence, and are influenced by, those of a collection of such molecules present in a solid material.[2]

The interplay between molecular and crystal structure is, of course, far more important when the molecule is intrinsically flexible. In such a case the crystal environment is not simply a spectator but participates in the definition of the molecular features. The construction of a system formed by flexible molecules in a crystal requires a global energy minimization in which the molecular and crystal structures are simultaneously optimized.[3]

With this idea in mind we have investigated several problems concerning the molecular and crystal structures of transition-metal complexes and clusters. Two powerful tools have been successfully practised: the structure of the isolated molecule can be investigated by extended-Hückel molecular-orbital calculations,[4] while the crystal structure and the organization and stability of the molecular assemblage can be studied by empirical atom–atom pairwise packing potential-energy calculations and computer graphics.[5]

In this paper we tackle the problem of the tetrahedral $[M_4(CO)_{12}]$ cluster complexes, where M = Co, Rh or Ir, and that of their neutral and ionic derivatives in which one or more carbonyls are replaced by other ligands. For tetrahedral cluster molecules of general formula $[M_4(CO)_nL_m]$ (where L can be mono- or poly-dentate ligands) two structural forms have been observed in solution: the 'all-terminal' structure with no bridging carbonyl ligands and the 'bridged' structure with three edge-bridging carbonyls spanning one tetrahedron face.[6] These two forms have been shown to interconvert *via* the so-called 'merry-go-round' carbonyl-exchange process.[7] Depending on the metal atom, however, $[M_4(CO)_nL_m]$ clusters and their substitution derivatives group in different classes as shown in Fig. 1. The results of a survey by means of the CSD[8] of all $[M_4(CO)_nL_m]$ compounds (M = Co, Rh or Ir) the structures of which have been determined by single-crystal diffraction methods are listed in Table 1.

With respect to the information shown in Fig. 1 and grouped in Table 1 the following general comments can be made: (*i*) $[Co_4(CO)_{12}]$[9] and $[Rh_4(CO)_{12}]$[21] crystallize in their 'bridged' (C_{3v} idealized symmetry) isomeric form whereas $[Ir_4(CO)_{12}]$ is known in the 'all-terminal' (T_d idealized symmetry) form;[29] (*ii*) all derivatives of $[Co_4(CO)_{12}]$ and $[Rh_4(CO)_{12}]$ characterized to date maintain the 'bridged' distribution of carbonyl ligands irrespective of the type of ligand and of the presence of an ionic charge; (*iii*) depending on the type of ligand, on the contrary, $[Ir_4(CO)_{12}]$ derivatives have been found as both 'all-terminal' and 'bridged' forms, although this latter is by far more abundant.

Some details of the molecular structures of these complexes also deserve attention. The M–M bond lengths for bridged and unbridged bonds, as well as the distances for terminal and bridging carbonyls respectively, are compared in Table 1. The molecular structural features can be summarized as follows: (*a*) for cobalt clusters CO-bridged M–M bonds are invariably *shorter* than the unbridged bonds, the average difference $\Delta = [(M\text{–}M)_{nb} - (M\text{–}M)_b]$ being 0.059 Å; (*b*) for cluster derivatives of Rh and Ir, on the contrary, CO-bridged M–M bonds are *longer* with respect to the unbridged bonds {average differences $\Delta = [(M\text{–}M)_{nb} - (M\text{–}M)_b]$ are −0.044 and −0.024 Å for M = Rh and Ir, respectively}; (*c*) in the case of Ir, those derivatives that preserve the all-terminal structure of the parent molecule show systematically shorter M–M bonds with respect to derivatives in the bridged form; (*d*) this applies also to the two cases for which both forms could be isolated and characterized in the solid state, namely the neutral species $[Ir_4(CO)_9\{\mu_3\text{-}(SCH_2)_3\}]$ [$(SCH_2)_3$ = 1,3,5-trithiacyclohexane][48] and the ionic cluster $[Ir_4(CO)_{11}(SCN)]^-$.[51]

The relationship between M–M bond length and the presence of bridging ligands, as well as the crystal structure of the two pairs of isomers mentioned above have been partially discussed in previous papers.[54,55]

The crystal structure problem related to these clusters can be summarized as follows: (*i*) bridging carbonyl ligands have been demonstrated to form CH···OC bonding interactions which are stronger than those established by terminal ligands,[56] *viz.*

† *Non-SI unit employed:* eV ≈ 1.60 × 10^{-19} J.

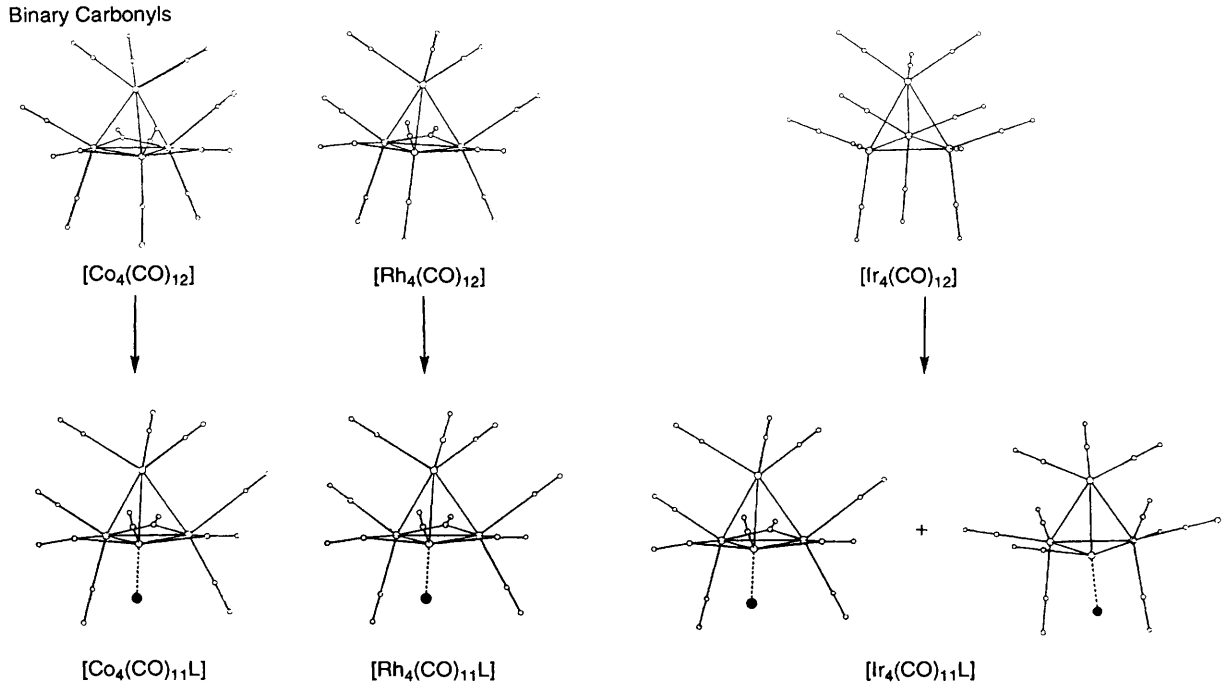

Fig. 1 Main structural forms observed in the solid state for $[M_4(CO)_{12}]$ (M = Co, Rh or Ir) clusters and their substitution derivatives

crystals of bridged clusters are favoured over those of compounds carrying only terminal ligands if CH···OC interactions can be established; (*ii*) in charged species the effect of the counter ion choice must also be taken into account;[57] it has been shown in the case of low- and high-nuclearity clusters that the size, shape and charge of the cations can influence not only the structure of the cations but also the inter-ion organization in the crystal structure.

Given these premises, it should be clear that this family of complexes still offers matters of investigation. With this paper we will try to address the following questions: (*a*) is it possible to understand the nature of factors which lead to a stabilization of the terminal structure in the iridium complexes?; (*b*) which factors will favour the existence of the two isomers in the two cases where they have been observed [$(SCH_2)_3$ and SCN^- as ligands]?; (*c*) what is the *electronic* reason for the different behaviour of the M–M bond lengths upon bridge formation in the case of Co with respect to Rh and Ir?; why do all Ir–Ir bonds lengthen on passing from an unbridged to a bridged distribution of carbonyl ligands?; (*d*) is there a relationship between the isolation of different isomeric forms and the network of intermolecular interactions established in the solid state?; (*e*) is there a recognizable effect of the ionic charge on the patterns of intermolecular CH···OC interactions between anions and cations?

Molecular Orbital Calculations

Tetranuclear clusters constitute an important class of clusters, which has been widely studied.[58–60] Three different geometries have been calculated for the family of compounds $[M_4(CO)_{12}]$ (M = Co, Rh or Ir), the more symmetric T_d one, observed only for Ir, the C_{3v} one, seen for both Co and Rh, and the unknown D_{2d} one.[60b] The bonding mode was examined, but the questions being handled were very different from those we have listed above, as much more is now known about these clusters and their structures. As shown in Table 1, the monosubstituted derivatives of $[Ir_4(CO)_{12}]$, $[Ir_4(CO)_{11}X]$, constitute a nice series in which both distributions of carbonyl ligands are observed. The terminal structure is observed for X = CO and CNBu^t, while the bridging one is more common (X = Br, I, phosphine, *etc.*). In the case of the thiocyanate ligand the two isomeric anions were isolated and their structures experimentally determined in the solid state by using different counter ions. This system will be mainly used in order to understand the reasons for the occurrence of carbonyl bridges. Another interesting cluster is the one where $(SCH_2)_3$ replaces three carbonyl groups. Again in this case two isomers were isolated, one containing only terminal carbonyls, the other also three bridging carbonyls.

The bridging structure seems to be the most common and the above results lead us to think that strong π-acceptor ligands may stabilize the terminal structure, though only for iridium. This result is analogous to that found for the triad of ruthenium clusters, $[Ru_3(CO)_9L]$, where L could be benzene, $(SCH_2)_3$ or $(CO)_3$.[61] The all-terminal structure was found both for benzene and the three carbonyls, and the bridged one in the $(SCH_2)_3$ case.

Extended-Hückel calculations were carried out on the two basic structures: the terminal and the one containing bridges (details are given in the Appendix). Four ligands were considered as replacing one carbonyl in the parent structure: PH_3, CNH, Br^- and SCN^-, leaving five pairs of compounds. Another sixth pair consists of the two $(SCH_2)_3$ clusters.

The simplest indicator of the stability of each form would be the total energy. One problem arises, however, because the number of bonds is greater in the fragment containing bridges, $[Ir_4(\mu\text{-}CO)_3(CO)_8]$, than in the terminal. Even taking into account that the Ir–C bonds are longer (and weaker) for the bridging carbonyl, the first fragment is much more stable in the extended-Hückel calculations and thus biases all the remaining results. For this reason, we started by looking at two other indicators, which were calculated assuming a decomposition of the cluster into two fragments, X and the $Ir_4(CO)_{11}$ group [or, for the $(SCH_2)_3$ clusters, $(SCH_2)_3$ and $Ir_4(\mu\text{-}CO)_3(CO)_6$ or $Ir_4(CO)_9$]. The first indicator is the interaction or binding energy, ΔE, defined as the difference between the energy of the cluster and the sum of the energies of the isolated fragments. This binding energy will, in principle, be larger (more negative) when the most stable structure is formed. The other probe is the overlap population between the two fragments. Overlap populations between atoms scale as bond strengths and the

Table 1 Comparison of averaged structural parameters for substituted derivatives of $[M_4(CO)_{12}]$ species (M = Co, Rh or Ir)

Complex	$(M–M)_{nb}$	$(M–M)_b$ [a]	Δ [b]	$M–C_t$	$M–C_b$	Ref.
$[Co_4(CO)_{12}]$ [c]	2.494(14)	2.485(12)	0.009	1.87(5)	2.06(5)	9
$[Co_4(\mu\text{-}CO)_3(CO)_8(PPh_3)]$	2.530(1)	2.482(1)	0.048	1.797(5)	1.937(4)	10
$[Co_4(\mu\text{-}CO)_3(CO)_8(PMe_3)]$	2.530(2)	2.496(2)	0.061	*d*	*d*	11
$[Co_4(\mu\text{-}CO)_3(CO)_7\{P(OMe)_3\}_2]$	2.528(1)	2.454(1)	0.074	1.784(7)	1.929(6)	10
$[Co_4(\mu\text{-}CO)_3(CO)_7\{PMe_2(CH_2CH_2CHCH_2)\}]$	2.52(1)	2.47(3)	0.048	1.78(3)	1.94(5)	12
$[Co_4(\mu\text{-}CO)_3(CO)_9(\eta^6\text{-}C_6H_6)]$	2.485(1)	2.457(2)	0.028	1.78(1)	1.948(9)	13
$[Co_4(\mu\text{-}CO)_3(CO)_3(\eta^6\text{-}C_6H_5Me)\{\mu_3\text{-}HC(PPh_2)_3\}]$	2.471(3)	2.447(3)	0.025	1.75(2)	1.91(2)	14
$[Co_4(\mu\text{-}CO)_3(CO)_6\{\mu_3\text{-}HC(PPh_2)_3\}]$	2.540(2)	2.457(2)	0.086	1.77(2)	1.93(1)	15
$[Co_4(\mu\text{-}CO)_3(CO)_9(\eta^6\text{-triptycene})]$ [e]	2.500	2.462	0.038	1.786	1.940	16
$[Co_4(\mu\text{-}CO)_3(CO)_5(PMe_3)\{\mu_3\text{-}HC(PPh_2)_3\}]$	2.529(3)	2.484(2)	0.045	1.74(1)	1.93(1)	17
$[Co_4(\mu\text{-}CO)_3(CO)_4(dppm)\{\mu_3\text{-}HC(PPh_2)_3\}]$ [f]	2.541(2)	2.460(2)	0.081	1.77(1)	1.93(1)	17
$[Co_4(\mu\text{-}CO)_3(CO)_4(PMe_3)_2\{\mu_3\text{-}HC(PPh_2)_3\}]$	2.550(4)	2.454(3)	0.096	1.78(3)	1.93(2)	17
$[Co_4(\mu\text{-}CO)_3(CO)_7\{\mu\text{-}(PhO)_2PN(Et)P(PhO)_2\}]$	2.534	2.441	0.093	1.749	1.920	18
$[Co_4(\mu\text{-}CO)_3(CO)_8\{C(O)Me\}]^-$	2.562(1)	2.461(1)	0.101	1.78(4)	1.94(4)	19
$[Co_4(\mu\text{-}CO)_3(CO)_8I]^-$	2.521(2)	2.467(2)	0.054	1.76(1)	1.94(1)	20
$[Rh_4(CO)_{12}]$ [c]	2.715(8)	2.749(8)	−0.034	1.96(7)	1.99(7)	21
$[Rh_4(\mu\text{-}CO)_3(CO)_7(PPh_3)_2]$	2.707(2)	2.750(2)	−0.043	1.88(7)	2.09(2)	22
$[Rh_4(\mu\text{-}CO)_3(CO)_6\{P(OPh)_3\}_3]$	2.694(2)	2.719(2)	−0.025	1.85(3)	2.06(2)	22
$[Rh_4(\mu\text{-}CO)_3(CO)_5\{P(OPh)_3\}_4]$	2.709(8)	2.741(8)	−0.032	1.83(6)	2.00(6)	23
$[Rh_4(\mu\text{-}CO)_3(CO)_5(dppm)_2]$	2.706(1)	2.715(1)	−0.009	1.91(2)	2.09(2)	24
$[Rh_4(\mu\text{-}PPh_2)_4(\mu\text{-}CO)_3(CO)_2(PPh_3)]$ [c]	*g*	2.876(2)	—	*d*	*d*	25
$[Rh_4(\mu\text{-}PPh_2)_4(\mu\text{-}CO)_2(CO)_4]$						26
monoclinic [c]	*g*	2.816(1)	—	1.86(7)	2.08(6)	
triclinic [c]	*g*	2.828(1)	—	*d*	*d*	
$[Rh_4(\mu\text{-}CO)_4(CO)_4\{P(OEt)_3\}]$	2.681(2)	2.785(2)	−0.104	1.87(2)	2.06(2)	27
$[Rh_4(\mu\text{-}CO)_3(CO)_8(PPr^i_3)]$	2.706(3)	2.762(2)	−0.054	1.93(2)	2.11(2)	28
$[Ir_4(CO)_{12}]$ [c]	2.693(7)	—	—	1.87	—	29
$[Ir_4(\mu\text{-}CO_2)(CO)_9(\mu\text{-}SO_2)]$	2.694(1)	2.731(3)	−0.037	1.93(2)	2.11(2)	30
$[\{Ir_4(\mu\text{-}CO)_3(CO)_8\}_2]^{2-}$	2.721(1)	2.752(1)	−0.031	1.88(2)	2.13(2)	31
$[Ir_4H(\mu\text{-}CO)_3(CO)_8]$						32
X-ray	2.706(2)	2.727(2)	−0.021	1.84(2)	1.98(5)	
neutron	2.714(1)	2.736(1)	−0.022	1.894(6)	2.02(2)	
$[Ir_4(\mu\text{-}CO)_3(CO)_8Br]^-$	2.696(1)	2.725(1)	−0.029	1.89(3)	2.10(3)	33
$[Ir_4(\mu\text{-}CO)_3(CO)_8(CO_2Me)]^-$	2.726(2)	2.717(2)	−0.009	2.00(6)	2.14(4)	34
$[\{(OC)_8(OC\text{-}\mu)_3Ir_4(PhPPPh)Ir_4(\mu\text{-}CO)(CO)_8(AuPEt)_3\}_2]$	2.711(2)	2.746(2)	−0.035	*d*	*d*	35
$[Ir_4(\mu\text{-}CO)_3(CO)_7(dmpe)]$ [h]	2.736(2)	2.739(2)	−0.003	1.84(3)	2.07(2)	36
$[Ir_4(\mu\text{-}CO)_3(CO)_7(pdma)]$ [i]	2.726(1)	2.720(2)	0.006	1.88(3)	2.11(3)	37
$[Ir_4(\mu\text{-}CO)_3(CO)_7(diop)]$ [j]	2.723(2)	2.764(2)	−0.041	1.84(3)	2.07(3)	38
$[Ir_4(\mu\text{-}CO)_3(CO)_6(PMe_2Ph)(nbd)]$ [k]	2.726(1)	2.720(1)	0.006	1.89(3)	2.07(2)	39
$[Ir_4(\mu\text{-}CO)_3(CO)_6(PPh_3)\{Ph_2P(CH_2)_3PPh_2\}]$	2.728(1)	2.745(1)	−0.017	1.84(2)	2.07(2)	40
$[Ir_4(\mu\text{-}CO)_3(CO)_5(PMe_3)_4]$	2.737(1)	2.745(1)	−0.008	1.85(2)	2.10(2)	41
$[Ir_4(\mu\text{-}CO)_3(CO)_5(dppm)]$	2.726(1)	2.725(1)	0.001	1.86(2)	2.12(2)	42
$[Ir_4(\mu\text{-}CO)_3(CO)_5(dppen)_2]$ [l]	2.686(2)	2.752(2)	−0.039	1.89(4)	2.05(4)	43
$[Ir_4H(\mu\text{-}CO)_3(CO)_4(dppen)(PhC_6H_4PC_2H_2PPh_2)]$ [c]	2.757(1)	2.719(1)	0.038	1.83(3)	2.07(3)	43
$[Ir_4(\mu\text{-}CO)_3(CO)_5(PPhMe_2)_4]$	2.730(3)	2.748(3)	−0.018	1.77(5)	2.07(5)	44
$[Ir_4H_2(\mu\text{-}CO)_3(CO)_7]^{2-}$ [c]	2.789(2)	2.711(2)	0.078	1.80(4)	2.03(3)	45
$[Ir_4(\mu_3\text{-}PPh)(\mu\text{-}CO)_3(PPh_3)_4]$	2.894(1)	2.747(1)	0.147	1.85(1)	2.09(1)	46
$[Ir_4(\mu_3\text{-}CO)_3(CO)_7(PPh_3)_2]$	2.726	2.751	−0.025	1.821	2.066	47
$[Ir_4(\mu_3\text{-}CO)_3(CO)_7(cod)]$ [m]	2.715(1)	2.737(1)	−0.022	1.91(2)	2.11(2)	48
$[Ir_4(\mu_3\text{-}CO)_3(CO)_7(CH_2CO_2Me)]^-$						49
molecule 1	2.722(2)	2.728(2)	−0.006	1.83	2.10(4)	
molecule 2	2.725(2)	2.730(2)	−0.005	1.81	2.07(4)	
$[Ir_4(\mu_3\text{-}CO)_3(CO)_8(CH_2CO_2Me)_2]^{2-}$	2.750(1)	2.725(1)	0.025	1.86	2.09(1)	49
$[Ir_4(\mu_3\text{-}CO)_3(CO)_7\{\mu\text{-}Ph_2P(CH_2)_4PPh_2\}]$	2.716(1)	2.745(1)	−0.029	1.87(3)	2.11(3)	50
$[Ir_4(\mu_3\text{-}CO)_3(CO)_8(SCN)]^-$	2.700(2)	2.721(2)	−0.021	1.90(3)	2.12(3)	51(*b*)
$[Ir_4(\mu\text{-}CO)_3(CO)_6\{\mu_3\text{-}(SCH_2)_3\}]$	2.680(2)	2.686(2)	−0.006	1.92(3)	2.11(3)	48
$[Ir_4(CO)_9\{\mu_3\text{-}(SCH_2)_3\}]$						48
molecule 1	2.655(2)	—	—	1.88(3)	—	
molecule 2	2.655(2)	—	—	1.88(3)	—	
$[Ir_4(CO)_9\{CH(PPh_2)_3\}]$	2.689(3)	—	—	*d*	—	52
$[Ir_4(CO)_{11}(CNBu^t)]$	2.685(1)	—	—	1.86(3)	—	53
$[Ir_4(CO)_{11}(SCN)]^-$	2.684(1)	—	—	1.91(2)	—	51(*a*)

[a] $\Delta = [(M–M)_{nb} - (M–M)_b]$. [b] Only CO-bridged M–M bonds were averaged. [c] Not included in the comparison because of the presence of other bridging ligands (such as hydrides) along the M–M bonds or because of disorder. [d] Not reported. [e] Triptycene = 9,10-dihydro-9,10-*o*-benzenoanthracene. [f] dppm = $Ph_2PCH_2PPh_2$. [g] No unbridged M–M bonds. [h] dmpe = $Me_2PCH_2CH_2PMe_2$. [i] pdma = *o*-Phenylenebis(dimethylarsine). [j] diop = 4,5-Bis(diphosphinomethyl)-2,2-dimethyl-1,3-dioxolane. [k] nbd = Norbornadiene (bicyclo[2.2.1]hepta-2,5-diene). [l] dppen = 1,2-Bis(diphenylphosphino)ethylene. [m] cod = Cycloocta-1,5-diene.

same idea applies to those calculated between fragments. The results obtained are collected in Table 2.

It can be added that the total energy was calculated for the two isomeric anions with the thiocyanate ligand having the

Table 2 Binding energies (eV), overlap populations (o.p.s) between fragments and total energies (eV) for the pairs of compounds $[Ir_4(\mu\text{-}CO)_3(CO)_8X]$ and $[Ir_4(CO)_{11}X]$

Cluster	ΔE*	o.p.	Total energy
$[Ir_4(\mu\text{-}CO)_3(CO)_8Br]^-$	−0.633	0.312	−2791.65
$[Ir_4(CO)_{11}Br]^-$	−0.088	0.328	−2790.95
$[Ir_4(\mu\text{-}CO)_3(CO)_8(PH_3)]$	−0.471	0.471	−2805.44
$[Ir_4(CO)_{11}(PH_3)]$	−0.256	0.458	−2804.37
$[Ir_4(\mu\text{-}CO)_3(CO)_8(SCN)]^-$	−0.153	0.328	−2942.90
$[Ir_4(CO)_{11}(SCN)]^-$	−0.127	0.346	−2942.17
$[Ir_4(\mu\text{-}CO)_3(CO)_8(CNH)]$	−1.658	0.654	−2857.74
$[Ir_4(CO)_{11}(CNH)]$	−1.888	0.695	−2857.36
$[Ir_4(\mu\text{-}CO)_3(CO)_8(CO)]$	−0.007	0.818	−2863.57
$[Ir_4(CO)_{11}(CO)]$	−0.115	0.875	−2863.30
$[Ir_4(\mu\text{-}CO)_3(CO)_6\{(SCH_2)_3\}]$	−3.585	1.266	−2874.72
$[Ir_4(CO)_9\{(SCH_2)_3\}]$	−3.825	1.295	−2873.63

* $\Delta E = (E_X + E_{Ir\ frag}) - E_{cluster}$.

Table 3 Overlap populations between atoms in the two $[Ir_4(CO)_{12}]$ isomers

o.p.s	$[Ir_4(CO)_{12}]$	$[Ir_4(\mu\text{-}CO)_3(CO)_9]$
Ir–Ir	0.245	0.242
Ir–Ir (bridged by CO)	—	0.189
Ir–C_t	0.889	0.839,[a] 0.857,[b] 0.905[c]
Ir–C_b	—	0.515
C–O_t	1.169	1.121
C–O_b	—	1.192

[a] Basal axial. [b] Basal equatorial. [c] Apical.

observed structure, using the coordinates experimentally obtained, the values being, respectively, −2943.667 eV for the bridging and −2942.625 eV for the terminal structure. These values are not and cannot be exactly the same as obtained with an idealized model, but they are comparable, both in their relative and their absolute value. Therefore the model essentially reproduces the behaviour of the clusters.

The data in Table 2 always show a larger, more negative, binding energy for the isomer which appears in the crystal structures, the bridging one for Br^-, PH_3, the terminal one for CNH and CO derivatives. In the case of the thiocyanate clusters, the binding energies are different, though not much. It should be added, however, that the conversion between the isomeric forms was studied in solution using NMR techniques and the bridging isomer was found to be the thermodynamic product.

Larger overlap populations between fragments reflect, for most cases, the formation of the more stable isomer. It is interesting that they are comparable for the two thiocyanate isomers. The total energies can be useful in a certain way: though the bridging species has always a lower energy than that of the terminal one [caused by the intrinsically lower energy of the bridging $Ir_4(CO)_{11}$ fragment, see below], they are comparable for CO and CNH (terminal isomer more stable), while for PH_3 and Br the difference increases dramatically (bridging form more stable).

The electronic reasons for this behaviour are related to the type of ligand: π-acceptor ligands, such as CO and CNH, stabilize the terminal structure, while π donors or strong σ donors without relevant π orbitals [Br^-, SCN^-, PH_3, $(SCH_2)_3$] favour the structure with bridges. The differences in energy and overlap populations are small and therefore difficult to show on an interaction diagram for this type of cluster containing many orbitals. As we discussed previously,[61] the cluster fragment having carbonyl bridges is less electron rich, owing to the better accepting power of the bridging carbonyls, and therefore less apt at co-ordinating ligands requiring electron-rich metal centres (carbonyl, isocyanide). We can trace this effect in the occupations of the carbonyl orbitals after co-ordination to $Ir_4(CO)_{11}$, to form the $[Ir_4(CO)_{12}]$ cluster. The π* orbitals receive 0.319 and 0.354 electron, but these numbers drop to 0.303 and 0.282 upon co-ordination to $Ir_4(\mu\text{-}CO)_3(CO)_8$. The difference in the occupation of the carbonyl donor orbital, its highest occupied molecular orbital (HOMO), is smaller for the terminal than for the bridging structure (residual populations are 1.635 *versus* 1.612). The co-ordinated carbonyl group acquires a charge of −0.115 when it is part of the terminal structure, but only −0.007 when it binds to the bridged moiety. This reflects the determining effect of the π-bonding component. When the ligands have no π-acceptor orbitals there is no electronic advantage of interacting with the less-stable terminal fragment. The fact that these differences are rather small allows an equilibrium situation to take place for some ligand/metal combinations, as observed for SCN^- and $(SCH_2)_3$.

The calculations were done using always the same average Ir–Ir distance (2.72 Å), although this bond length should be longer in bridged isomers than in the terminal ones (see Table 1). The overlap populations between iridium atoms inside the cluster reflect this behaviour, indicating that the Ir–Ir bonds should contract in the terminal isomers. As an example, the overlap populations for $[Ir_4(CO)_{12}]$ are given in Table 3.

The basal–basal Ir–Ir bonds, spanned by the carbonyl bridging ligands, have a much lower overlap population (0.189) and should therefore be longer than equatorial–apical bonds (overlap population 0.242) in the bridged isomer as generally observed. This trend is not observed for the lighter metal clusters of this family. In the calculations the metal–metal overlap population decreases and one would expect the distance to become longer, but it gets shorter. The problem of changes in distances in molecules of this complexity cannot be appropriately studied with extended-Hückel calculations and even with more quantitative methods. The reason for the different behaviour of cobalt with respect to rhodium and iridium lies in its contracted d orbitals which require short Co–C distances to form bonds with the bridging carbonyls in order to avoid very large M–C(O)–M angles. The same contracted d orbitals allow a close approach of the two metal atoms without involving extremely repulsive interactions.

The metal–carbonyl bonds are stronger for terminal carbonyls, and even more in $[Ir_4(CO)_{12}]$ than in $[Ir_4(\mu\text{-}CO)_3(CO)_9]$, except for the three Ir–C bonds in the apical $Ir(CO)_3$. Though the metal–carbonyl(bridging) bonds are weaker, there are two bonds per carbonyl group, and this greater number of bonds biases the total energy, giving the bridging isomer too low an energy, in this calculation method.

The C–O overlap populations are larger for the terminal carbonyls. As is well known from the metal–carbonyl bonding mode, back donation into the carbonyl π* orbital is larger for the bridging carbonyls, leading therefore to a weaker C–O bond. This effect is also reflected on the atomic charges of the oxygen atoms and these may be important in respect of intermolecular bonding. The oxygens of bridging carbonyls carry a charge of −0.83 *vs.* −0.72 for the terminal ones, while in the terminal isomer the oxygen charge is −0.74. These values vary slightly as one carbonyl ligand is replaced, but the trend is always the same. Interestingly, for both thiocyanate derivatives, the most negative charge is located on the nitrogen atom (−1.14).

Another feature of both thiocyanate clusters is the torsion of the SCN^- moiety away from the plane bisecting the basal Ir–Ir–Ir angle, which is significantly more pronounced in the bridging than in the terminal cluster. The potential-energy surfaces for these distortions are very soft, with minima at 45°

for the terminal isomer (0.02 eV) and at 55° for the bridging one (0.01 eV). These values suggest that these groups may easily bend in order to form intermolecular bonds, such as hydrogen bonds, involving the terminal nitrogen atom (see below). The energy of these bonds could be of the same order of magnitude, and their formation might in principle be the driving force for the distortion.

Tetranuclear rhodium complexes of the same kind have not been prepared and characterized in such large numbers. The only mono derivative is the phosphine complex $[Rh_4(\mu\text{-}CO)_3(CO)_8(PR_3)]$ and it has the same structure as that of the dodecacarbonyl cluster, which also presents three bridging carbonyls. There are more related compounds where more than two carbonyls have been substituted, but the same structure, with the $Rh_4(\mu\text{-}CO)_3$ motif, is always present. We show in Table 4 the results of the calculations performed on the two isomers of the two clusters.

The same indicators as in Table 1 (iridium compounds) have been adopted in Table 4. The binding energy, ΔE, again seems to be the most reliable one, suggesting the bridging structures are preferred for both clusters. The total energy gives the same result in this series of compounds. The overlap populations between fragments show the expected trend in the case of the phosphine ligand, while for the π-acceptor carbonyl derivative a stronger bond is formed when all the other carbonyls are terminal. Contrary to what is observed for the iridium clusters, the formation of the stronger bond is not enough to compensate for the lower stability of the non-bridged fragment. This is a general trend which is observed for similar carbonyl complexes of metals belonging to the same family. Bridged structures are generally observed in the carbonyl clusters of the lighter metals (see Table 1). As one moves down the family in the Periodic Table, the competition to form non-bridged structures becomes more effective: the two types of structures are observed for ruthenium,[61] the same being true of iridium, though only bridging clusters are known for rhodium, while for osmium terminal structures predominate.

This type of problem presents some difficulties when addressed using extended-Hückel calculations, though there have been attempts.[62] Fig. 2 illustrates the main interactions occurring when a carbonyl forms a bridge over two metal atoms. Diagrams **A** and **C** show the donation component. The molecular orbitals are both M–C and M–M bonding. On the other hand, the molecular orbitals resulting from back donation, **B** and **D**, are obviously M–C bonding, but also M–M antibonding. This means that the formation of the M–C bonds implies some repulsive metal–metal interaction. There will be a balance between their presence and that of extra M–C bonds: for light metals having contracted d orbitals, this repulsion will be minimal and formation of bridges prevails. As the metal d orbitals become more diffuse this antibonding interaction becomes stronger and bridges are less favoured. We discussed this effect in more detail for other systems[63] and there is a critical orbital which has been found to play a determining role. It is of type **B** or **D**, depending on the symmetry of the species being studied. Of course, the picture in Fig. 2 is a very simplified one. Suitable combinations of metal orbitals having the right symmetry to interact with carbonyl orbitals, either symmetric as in **A** and **C**, or antisymmetric as in **B** and **D** are found at different energies, occupied and unoccupied, according to how they are influenced by all the other cluster ligands. As mentioned above, the simultaneous presence in the cluster of strong σ- or π-donor ligands may sufficiently increase back donation (and therefore favour bridged carbonyls) to overcome this effect.[61]

Crystal Structure Analysis

We will now investigate the ion organization in the crystal structures of the charged species. Before proceeding, however, it is worth commenting on the difference between crystals formed

Table 4 Binding energies (eV), overlap populations between fragments, and total energies (eV) for the pairs of compounds $[Rh_4(\mu\text{-}CO)_3(CO)_8X]$ and $[Rh_4(CO)_{11}X]$

Cluster	ΔE*	o.p.	Total energy
$[Rh_4(\mu\text{-}CO)_3(CO)_8(PH_3)]$	−0.428	0.439	−2805.270
$[Rh_4(CO)_{11}(PH_3)]$	0.415	0.413	−2803.165
$[Rh_4(\mu\text{-}CO)_3(CO)_8(CO)]$	−2.154	0.727	−2862.597
$[Rh_4(CO)_{11}(CO)]$	−2.057	0.780	−2861.783

* $\Delta E = (E_X + E_{Rh\,frag}) - E_{cluster}$.

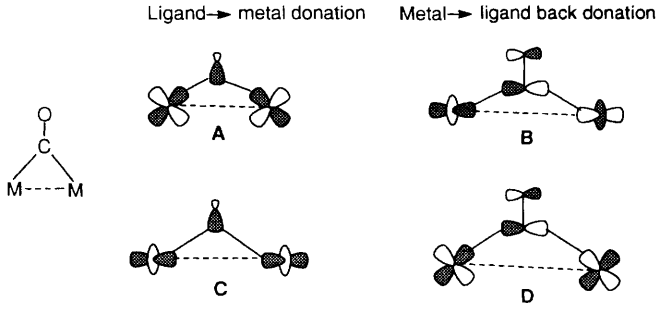

Fig. 2 Interaction between one bridging CO and two metal atoms

of neutral molecules and molecular salts formed by anionic clusters and their counter ions. Neutral molecules have been shown, in previous studies, to constitute typical, organic-type, molecular crystals.[64] In such crystals the crystal cohesion and intermolecular interlocking is controlled primarily by van der Waals interactions and hydrogen bonds of the CH···O type amongst the ligand peripheral atoms. Crystalline salts formed by high-nuclearity cluster anions and organic cations, on the other hand, have characteristics that recall closely those of molecular co-crystals[65] because the anionic charge is so much diffused over the whole cluster body as to be almost ineffective in controlling the packing arrangement.[2] There is, however, the definite possibility that, although the arrangement in the solid is chiefly controlled by the relative size and shape of the component ions, the presence of additional interactions, such as hydrogen bonds involving the carbonyl ligands, can pilot the packing choice amongst the various possible structures.[56]

In order to explore these possibilities we have calculated, for all isomeric pairs, van der Waals volumes and packing coefficients (p.c.), which are useful descriptors of molecular crystals.[66,67] The hydrogen-bonding network has also been explored by calculating the separations and angles between all possible donor and acceptor groups. Methods employed for this analysis are described in the Appendix. The molecular volumes calculated with the integration method are 364.9 Å^3 (p.c. = 0.71) for $[Ir_4(CO)_9\{\mu_3\text{-}(SCH_2)_3\}]$, 357.2 Å^3 (p.c. = 0.71) for $[Ir_4(\mu\text{-}CO)_3(CO)_6\{\mu_3\text{-}(SCH_2)_3\}]$, 351.4 Å^3 (p.c. = 0.64) for $[NMe_2(CH_2Ph)_2][Ir_4(CO)_{11}(SCN)]$ and 344.1 Å^3 (p.c. = 0.64) for $[N(PPh_3)_2][Ir_4(\mu\text{-}CO)_3(CO)_8(SCN)]$. From these data it appears that both bridged species possess a smaller volume than the all-terminal ones. This might seem to contrast with the fact that the Ir–Ir bonds in the bridged species are longer than in the unbridged ones, but is consistent with the fact that the bridging C atoms are embedded in the metal core. Furthermore it is interesting that the neutral species achieve a much denser packing than do the ionic species.

Cation–anion interactions in terms of the packing distribution of the ions and of hydrogen-bonding interactions of the CH···O type were studied for several ionic species presented in Table 1. The existence of networks of CH···O interactions between the hydrogen atoms of the cation and the carbonyl ligands of the metal clusters was revealed. As in the case of

previous studies, the hydrogens were in calculated positions, so attention was also given to the C···O distances.[56] The hydrogen bonds also appeared as repulsions in the partitioning of packing potential-energy calculations over the individual groups of intermolecular interactions. Table 5 lists the CH···O bonds shorter than 2.6 Å.

We observe that terminal and bridging carbonyls establish short CH···O separations. Both H···O and C···O distances are generally shorter for bridging than for terminal ligands. In addition to this well ascertained fact, CH···O intermolecular bonds are also appreciably shorter in crystalline salts than in the crystals formed by neutral species. In crystalline salts of the type discussed herein the interactions are between the carbonyl ligands of the anions and the H atoms belonging to the cations. These interactions are strengthened by the additional polarization arising from the net ionic charge delocalized over the clusters or the organic counter ions. It can be said that, although crystalline salts formed of cluster anions and organic cations behave essentially as binary or ternary co-crystals in which particles are packed according to close-packing rules, the ionic charge has the effect of 'piloting' amongst the large number of possible alternative ways to construct these co-crystals towards those which also optimize the intermolecular hydrogen bondings. Table 5 also shows that the preference for hydrogen bonds with the bridging ligands with respect to terminal ones is not a hard and fast rule, rather a general trend of these and other complexes of this type. When terminal ligands are preferred, it may well be because that maximization of the number of hydrogen bonds is more important than the type of carbonyl involved.

Let us examine the cases listed in Table 5 in more detail. In crystalline $[PPh_4][Co_4(\mu\text{-}CO)_3(CO)_8(COMe)]$ the shortest CH···O interaction (2.385 Å) is established by the COMe group and the cation hydrogen atoms. The terminal CO(41) is involved in a similar interaction (2.399 Å). The remaining interactions are distributed over a narrow range (2.418–2.582 Å) with the bridging carbonyls having the smaller values. A grand total of 10 CH···O interactions form a web around the PPh_4^+ cations. The situation is different in crystalline $[NEt_4][Co_4(\mu\text{-}CO)_3(CO)_8I]$ where the only short CH···O contact is 2.526 Å. This distance is much longer than those discussed above although it involves a bridging carbonyl ligand, and reflects the difference in acidity of the aliphatic H atoms in the NEt_4^+ cation with respect to the phenyl H atoms in the PPh_4^+ cation. Crystalline $[P(CH_2Ph)Ph_3][Ir_4H(\mu\text{-}CO)_2(CO)_9]$ presents very short CH···O intermolecular bonds involving the bridging CO(231). The shortest interaction (2.191 Å) is with the benzylic hydrogen H(501), whereas the shortest distance from a phenyl hydrogen is 2.281 Å. The bridging CO(231) is actually involved in a trifurcated interaction with the cation, as shown in Fig. 3. The H atoms of the cation are involved in 12 interactions below 2.6 Å. There is no indication of involvement of the H(hydride) atom in short intermolecular contacts. The bromide cluster $[PPh_4][Ir_4(\mu\text{-}CO)_3(CO)_8Br]$ shows the presence of a very short CH···O intermolecular bond (2.273 Å) between one phenyl H atom and the bridging CO(9) thus forming a sort of ion pair as depicted in Fig. 4. In crystalline $[NMe_2(CH_2Ph)_2][Ir_4(\mu\text{-}CO)_3(CO)_8(CO_2Me)]$ the shortest interaction (2.378 Å) involves a terminal ligand, while the bridging carbonyls participate in a more extensive network of hydrogen bonds. The oxygen atom of the CO_2Me group, on the contrary, does not participate in any such interaction.

We now describe together the two isomers $[NMe_2(CH_2Ph)_2][Ir_4(CO)_{11}(SCN)]$ and $[N(PPh_3)_2][Ir_4(CO)_3(CO)_8(SCN)]$ which, as discussed above, represent, together with the pair of neutral molecules $[Ir_4(CO)_{11}\{\mu_3\text{-}(SCH_2)_3\}]$ and $[Ir_4(\mu\text{-}CO)_3(CO)_8\{\mu_3\text{-}(SCH_2)_3\}]$, the only example of isomeric pairs characterized in this family of compounds. Though the packing arrangement was discussed previously,[55] hydrogen-bonding interactions were not analysed. We now find that there

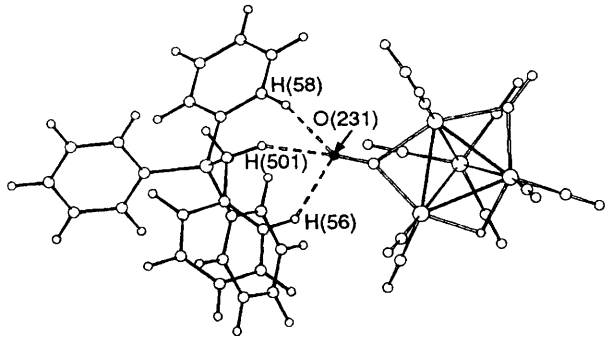

Fig. 3 Network of CH···O interactions enclosing the $[P(CH_2Ph)Ph_3]^+$ cation in crystalline $[P(CH_2Ph)Ph_3][Ir_4H(\mu\text{-}CO)_2(CO)_9]$

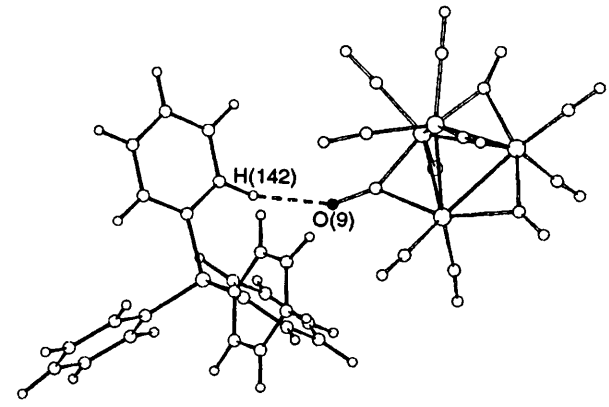

Fig. 4 Shortest interaction in crystalline $[PPh_4][Ir_4(\mu\text{-}CO)_3(CO)_8Br]$

is a marked difference between the two crystal structures. In both crystals there are short CH···O interactions involving terminal ligands: C(111)–H(112)···O(32) 2.328 in $[NMe_2(CH_2Ph)_2][Ir_4(CO)_{11}(SCN)]$; C(17)–H(17)···O(11) 2.395 Å in $[N(PPh_3)_2][Ir_4(CO)_3(CO)_8(SCN)]$ and a diffuse network involving both the bridging and the other terminal ligands. The nitrogen atoms of the thiocyanate groups, on the other hand, behave differently: in $[NMe_2(CH_2Ph)_2][Ir_4(CO)_{11}(SCN)]$ the N atom interacts with a methylenic hydrogen of the $[NMe_2(CH_2Ph)_2]^+$ cation [C(311)–H(311)···N(11) 2.281 Å] and more weakly with a phenyl hydrogen atom [2.699 Å, C(415)–H(415)···N(11)]; in crystalline $[N(PPh_3)_2][Ir_4(CO)_3(CO)_8(SCN)]$, on the other hand, the N atom participates in three interactions, all involving phenyl H atoms, in the range 2.415–2.616 Å. These two groups of interactions are depicted in Fig. 5 which shows how the torsion of the thiocyanate group allows maximization of the number of CH···N hydrogen bonds. This observation is in keeping with the results of our calculations discussed in the previous section and allows one to conclude that the orientation of the thiocyanate plays a role in determining the stability of the unbridged isomer.

Conclusion

With this paper we have analysed a large family of transition-metal clusters in terms of the structure of the isolated molecular systems and of that of their solids. As far as this latter aspect is concerned our attention has been focused on the arrangement and inter-ion interactions in the crystals formed by the ionic species in the family. We have made use of methods previously applied with success to a number of problems concerning the relationship between the molecular and crystal structures of structurally non-rigid organometallic molecules. This problem

Table 5 Relevant structural parameters (distances in Å, angles in °) for the C–H · · · O and C–H · · · N hydrogen bonds between anions and cations in the ionic species (T = terminal, E = edge-bridging CO)

Type	C–H · · · O/N	C · · · O/N	H · · · O/N	C–H · · · O/N
$[PPh_4][Co_4(\mu\text{-}CO)_3(CO)_8(COMe)]$				
E	C(113)–H(113) · · · O(5)	3.494	2.488	154.5
E	C(114)–H(114) · · · O(6)	3.382	2.418	148.0
T	C(114)–H(114) · · · O(13)	3.260	2.575	120.6
E	C(116)–H(116) · · · O(7)	3.532	2.568	148.1
T	C(132)–H(132) · · · O(12)	3.179	2.428	125.5
T	C(134)–H(134) · · · O(41)	3.431	2.399	159.3
T	C(135)–H(135) · · · O(42)	3.372	2.385	151.3
T	C(143)–H(143) · · · O(42)	3.453	2.582	137.2
E	C(144)–H(144) · · · O(6)	3.413	2.539	137.4
E	C(145)–H(145) · · · O(7)	3.432	2.469	147.8
$[NEt_4][Co_4(\mu\text{-}CO)_3(CO)_8I]$				
E	C(9)–H(3) · · · O(7)	3.596	2.526	170.9
$[P(CH_2Ph)Ph_3][Ir_4H(\mu\text{-}CO)_2(CO)_9]$				
T	C(54)–H(54) · · · O(23)	3.312	2.527	128.7
T	C(54)–H(54) · · · O(13)	3.225	2.454	127.2
E	C(56)–H(56) · · · O(231)	3.382	2.451	143.7
E	C(58)–H(58) · · · O(231)	3.299	2.281	156.4
T	C(60)–H(60) · · · O(21)	3.321	2.595	124.0
T	C(66)–H(66) · · · O(15)	3.239	2.506	124.2
T	C(66)–H(66) · · · O(43)	3.336	2.593	125.3
T	C(68)–H(68) · · · O(15)	3.421	2.584	133.7
E	C(68)–H(68) · · · O(241)	3.480	2.522	147.2
T	C(74)–H(74) · · · O(31)	3.330	2.456	137.2
E	C(50)–H(501) · · · O(231)	3.182	2.191	151.4
E	C(50)–H(502) · · · O(241)	3.570	2.516	164.9
$[PPh_4][Ir_4(\mu\text{-}CO)_3(CO)_8Br]$				
T	C(221)–H(122) · · · O(4)	3.517	2.594	142.9
E	C(421)–H(142) · · · O(9)	3.325	2.273	164.0
$[NMe_2(CH_2Ph)_2][Ir_4(\mu\text{-}CO)_3(CO)_8(CO_2Me)]$				
T	C(60)–H(61) · · · O(31)	3.421	2.500	142.6
T	C(60)–H(61) · · · O(55)	3.237	2.476	126.5
T	C(62)–H(62) · · · O(13)	3.437	2.488	146.0
T	C(70)–H(70) · · · O(31)	3.375	2.412	147.8
T	C(70)–H(71) · · · O(51)	3.422	2.430	152.1
T	C(72)–H(72) · · · O(51)	3.455	2.485	148.9
T	C(74)–H(74) · · · O(13)	3.477	2.579	140.1
T	C(75)–H(75) · · · O(55)	3.468	2.432	160.3
T	C(80)–H(81) · · · O(31)	3.447	2.516	143.8
T	C(80)–H(82) · · · O(53)	3.075	2.378	120.8
$[PPh_4]_2[Ir_4(\mu\text{-}CO)_3(CO)_7\{CH_2(CO_2Me)_2\}]$				
T	C(21)–H(4) · · · O(6)	3.504	2.523	150.6
T	C(22)–H(5) · · · O(3)	3.374	2.592	128.6
T	C(24)–H(6) · · · O(7)	3.488	2.474	155.9
E	C(25)–H(7) · · · O(9)	3.482	2.437	162.5
T	C(26)–H(8) · · · O(8)	3.500	2.599	140.5
T	C(33)–H(14) · · · O(7)	3.469	2.552	142.2
T	C(39)–H(19) · · · O(2)	3.534	2.474	166.8
E	C(48)–H(26) · · · O(12)	3.549	2.528	157.4
E	C(50)–H(28) · · · O(10)	3.359	2.458	140.2
T	C(50)–H(28) · · · O(14)	3.103	2.464	116.7
T	C(51)–H(29) · · · O(14)	3.023	2.362	118.0
T	C(55)–H(32) · · · O(8)	3.237	2.596	117.3
T	C(57)–H(34) · · · O(11)	3.258	2.592	119.2
$[NMe_2(CH_2Ph)_2][Ir_4(CO)_{11}(SCN)]$				
T	C(111)–H(111) · · · O(31)	3.334	2.575	126.6
T	C(111)–H(112) · · · O(32)	3.376	2.328	163.1
T	C(211)–H(211) · · · O(21)	3.519	2.493	158.3
T	C(311)–H(311) · · · N(11)	3.329	2.281	163.1
T	C(313)–H(313) · · · O(42)	3.502	2.508	152.6
T	C(413)–H(413) · · · O(23)	3.334	2.472	135.9

Table 5 (*continued*)

Type	C–H · · · O/N	C · · · O/N	H · · · O/N	C–H · · · O/N
$[N(PPh_3)_2][Ir_4(\mu\text{-}CO)_3(CO)_8(SCN)]$				
Intra	C(13)–H(13) · · · N(2)	3.045	2.564	106.0
T	C(15)–H(15) · · · N(1)	3.371	2.415	146.7
T	C(17)–H(17) · · · O(11)	3.455	2.395	166.8
Intra	C(25)–H(25) · · · N(2)	2.882	2.431	103.5
T	C(26)–H(26) · · · S(1)	3.780	2.766	156.3
E	C(28)–H(28) · · · O(8)	3.411	2.543	136.8
E	C(34)–H(34) · · · O(9)	3.274	2.517	126.3
T	C(37)–H(37) · · · N(1)	3.509	2.505	154.1
Intra	C(41)–H(41) · · · N(2)	3.070	2.577	106.9
Intra	C(43)–H(43) · · · N(2)	2.980	2.497	105.9
T	C(46)–H(46) · · · O(6)	3.339	2.435	140.5

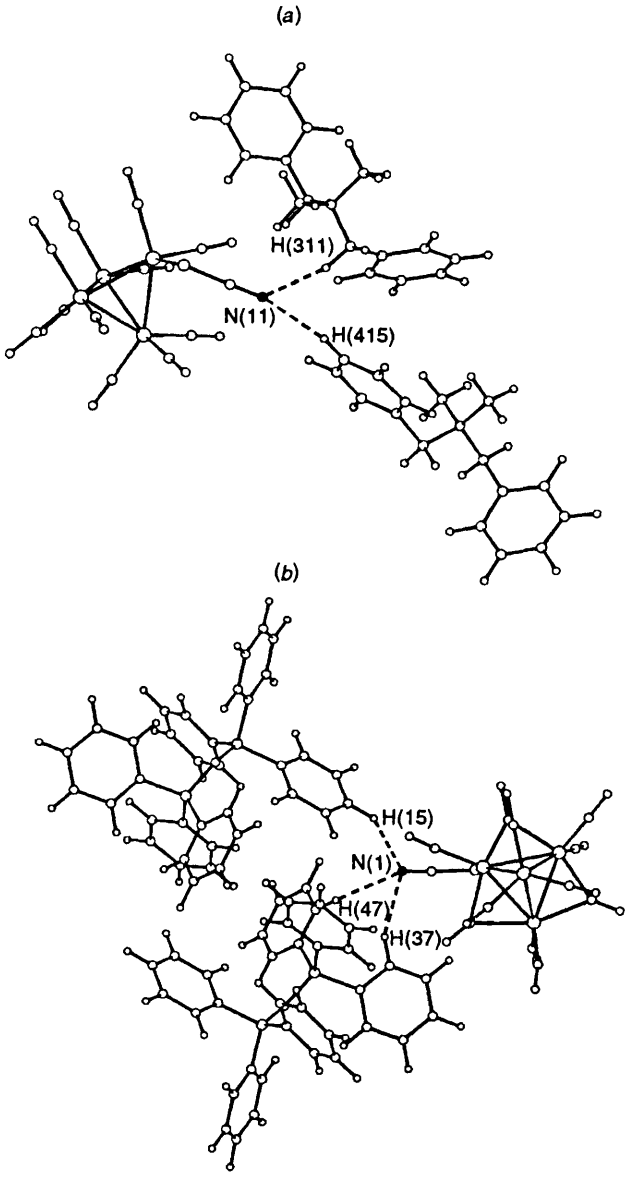

Fig. 5 The CH · · · N interactions in crystalline $[NMe_2(CH_2Ph)_2][Ir_4(CO)_{11}(SCN)]$ (*a*) and $[N(PPh_3)_2][Ir_4(CO)_3(CO)_8(SCN)]$ (*b*)

is particularly relevant for neutral and ionic derivatives of $[M_4(CO)_{12}]$ clusters (M = Co, Rh or Ir) because of the difference between the two major isomeric forms available, namely the 'all-terminal' (isolated in the solid state only for M = Ir) and the 'bridged' form known for all three metals. In the case of iridium, the two forms have been both isolated and structurally characterized in their crystals. This has offered the opportunity for a close comparison not only in terms of the molecular structures but also of the respective crystals. Our observations can be summarized as follows.

(*i*) Extended-Hückel calculations have indicated that, since bridging carbonyls are more efficient π acceptors than are terminal ones, their presence is favoured in the absence of strong π-acceptor ligand(s), such as CO. Hence π-acceptor ligands, such as CO and CNH, stabilize the terminal structure, while π donors or strong σ donors without relevant π orbitals [Br^-, SCN^-, PH_3, $(SCH_2)_3$] favour the structure with bridging carbonyls.

(*ii*) The differences in energy and overlap populations between the two forms are, however, generally small and equilibrium situations can be found for some ligands, as observed for SCN^- and $(SCH_2)_3$ bound to iridium clusters. In these cases the isolation and separate characterization of the isomers is possible (see below).

(*iii*) In bridged iridium (and rhodium) clusters, the basal–basal metal–metal bonds are longer than equatorial–apical bonds and have a much lower overlap population. In cobalt clusters the contracted d orbitals enforce a close approach of the two metal atoms while forming bonds to bridging carbonyls, but do not lead to strong repulsive interactions.

(*iv*) In the thiocyanate iridium clusters the SCN^- ligand can rotate over a rather flat potential-energy surface with minima at 45° for the terminal isomer and at 55° for the bridging one (0.02 and 0.01 eV, respectively). The difference in energy is small enough to be comparable to that of intermolecular interactions with the counter ions. We suggest that the counter ions $[NMe_2(CH_2Ph)_2]^+$ and $[N(PPh_3)_2]^+$, with their different steric requirements, favour different orientations of the SCN ligand, and therefore stabilize the bridged or the all-terminal structure *via* the formation of C–H · · · N hydrogen bonds.

(*v*) The interaction between large monoanionic M_4 clusters and cations carrying a small charge in the crystal structure is primarily controlled by the relative size and shape of the component ions. However, more directional, though weak, interactions such as those established between carbonyl ligands and C–H donors present on the cations, also play an important role. It would appear that this role is mainly that of selecting amongst various alternative ways to pack together efficiently anionic clusters and organic type cations, the one(s) which also optimize inter-ion interactions by taking advantage of the additional cohesion afforded by CH · · · O interactions. With this idea in mind we have been able to prepare crystalline materials in which the paramagnetic $Cr(C_6H_6)_2^+$ cation interacts with a complex monoanionic system formed by three cyclohexanedione molecules and one enolate anion *via* C–H · · · O interactions.[68]

Appendix

All the molecular-orbital calculations were done using the extended-Hückel method[4] with modified H_{ij}s.[69] The basis set for the metal atom consisted of *n*s, *n*p and (*n* − 1)d orbitals. Only 3s and 3p orbitals were considered for sulfur and phosphorus. The s and p orbitals were described by single Slater-type wavefunctions, and the d orbitals taken as contracted linear combinations of two Slater-type wavefunctions. Standard parameters were used for H, C, N, O, Br, P and S, while those for Ir were (H_{ij}/eV, ζ) 6s, −11.30, 2.504; 6p, −4.50, 2.20; 5d, −12.10, 5.796, 2.557 (ζ_2), 0.6351 (C_1), 0.5556 (C_2); and Rh (H_{ij}/eV, ζ) 5s, −8.09, 2.135; 5p, −4.57, 2.10; 4d, −12.50, 5.542, 2.39 (ζ_2), 0.5823 (C_1), 0.6405 (C_2). Three-dimensional representations of orbitals were drawn using the program CACAO.[70]

Idealized models having C_{3v} or T_d symmetry were used, respectively, for $[Ir_4(\mu\text{-}CO)_3(CO)_9]$ and $[Ir_4(CO)_{12}]$, and one CO was replaced by each monodentate ligand, X, as observed in the respective cluster type (see Table 1). For the terminal isomers the angles between the centre of the tetrahedron, Ir and C were optimized to 114°. This angle had this same value for the apical $Ir(CO)_3$ group in the terminal clusters. The bridging carbonyl groups were kept in the Ir_3 basal plane, except for the $(SCH_2)_3$ derivative where they had to be moved 19° away from that plane and towards the apical site in order to avoid very strong repulsions with $(SCH_2)_3$. The two terminal substituents at each basal iridium atom were perpendicular to each other, the upper one rotated 22° above the basal plane. The CNH ligand used to model Bu^{t}NC was taken as linear and the H–P–H angle in the model phosphine was optimized. The following distances (Å) were used: Ir–Ir 2.72, Ir–C(terminal) 1.90, Ir–C(bridging) 2.10, C–O 1.15, Ir–S 2.455, S–C 1.65, C–N 1.15, Ir–Br 2.576, Ir–P 2.375, P–H 1.42, N–H 1.0 and Rh–Rh 2.70. The geometry of $(SCH_2)_3$ was idealized from that observed in the two structures containing it.

The volumes and packing coefficients were calculated by use of integration methods and the OPEC suite of programs;[71] PLATON was used to search for possible hydrogen bonds.[72] The distances reported in Table 5 are those shorter than 2.6 Å. The positions of the hydrogen atoms were normalized along the C–H vectors to a neutron-derived value of 1.08 Å. The program SCHAKAL was used for the graphical representation of the results.[73]

Acknowledgements

D. B., F. G. and M. J. C. acknowledge the Consiglio Nazionale delle Ricerche (Italy) and the Junta Nacional de Investigação Científica e Technológica (Portugal) for joint financial support. The ERASMUS exchange program 'Crystallography' is acknowledged for financing J. J. B.

References

1 D. Braga, P. J. Dyson, F. Grepioni, B. F. G. Johnson and M. J. Calhorda, *Inorg. Chem.*, 1994, **33**, 3218; F. Grepioni, D. Braga, P. Dyson, B. F. G. Johnson, F. M. Sanderson, M. J. Calhorda and L. Veiros, *Organometallics*, 1995, **14**, 121.
2 D. Braga and F. Grepioni, *Acc. Chem. Res.*, 1994, **27**, 51.
3 D. Braga, *Chem. Rev.*, 1992, **92**, 633.
4 R. Hoffmann, *J. Chem. Phys.*, 1963, **39**, 1397; R. Hoffmann and W. N. Lipscomb, *J. Chem. Phys.*, 1962, **37**, 2179.
5 D. Braga and F. Grepioni, *Organometallics*, 1992, **11**, 711; D. Braga, F. Grepioni and P. Sabatino, *J. Chem. Soc., Dalton Trans.*, 1990, 3137; D. Braga and F. Grepioni, *Organometallics*, 1991, **10**, 1254.
6 E. Band and E. L. Muetterties, *Chem. Rev.*, 1978, **78**, 639.
7 F. A. Cotton and B. E. Hanson, *Rearrangements in Ground and Excited States*, ed. P. De Mayo, Academic Press, New York, 1980, p. 379; J. W. Faller, *Adv. Organomet. Chem.*, 1978, **16**, 211.
8 F. H. Allen, S. Bellard, M. D. Brice, C. A. Cartwright, A. Doubleday, H. Higgs, T. Hummelink, B. J. Hummelink-Peters, O. Kennard, W. D. S. Motherwell, J. R. Rodgers and D. G. Watson, *Acta Crystallogr., Sect. B*, 1979, **35**, 2331; F. H. Allen, J. E. Davies, J. J. Galloy, O. Johnson, O. Kennard, C. F. Macrae and D. G. Watson, *J. Chem. Inf. Comput. Sci.*, 1991, **31**, 204.
9 P. Corradini, *J. Chem. Phys.*, 1959, **31**, 1676; F. H. Carré, F. A. Cotton and B. A. Frenz, *Inorg. Chem.*, 1976, **15**, 380.
10 D. J. Darensbourg and M. J. Incorvia, *Inorg. Chem.*, 1981, **20**, 1911.
11 K. Bartl, R. Boese and G. Schmid, *J. Organomet. Chem.*, 1981, **206**, 331.
12 E. Keller and H. Vahrenkamp, *Chem. Ber.*, 1981, **114**, 1111.
13 P. H. Bird and A. R. Fraser, *J. Organomet. Chem.*, 1974, **73**, 103.
14 A. A. Bahsoun, J. A. Osborn, C. Voelker, J.-J. Bonnet and G. Lavigne, *Organometallics*, 1982, **1**, 1114.
15 D. J. Darensbourg, D. J. Zalewski and T. Delord, *Organometallics*, 1984, **3**, 1210.
16 R. A. Gancarz, J. F. Blount and K. Mislow, *Organometallics*, 1985, **4**, 2028.
17 D. J. Darensbourg, D. J. Zalewski, A. L. Rheingold and R. L. Durney, *Inorg. Chem.*, 1986, **25**, 3281.
18 N. J. Bailey, G. deLeeuw, J. S. Field, R. J. Haines and I. C. D. Stuckenberg, *S. Afr. J. Chem.*, 1985, **38**, 139.
19 M. J. Went, C. P. Brock and D. F. Shriver, *Organometallics*, 1986, **5**, 755.
20 V. G. Albano, D. Braga, G. Longoni, S. Campanella, A. Ceriotti and P. Chini, *J. Chem. Soc., Dalton Trans.*, 1980, 1820.
21 C. H. Wei, *Inorg. Chem.*, 1969, **8**, 2384.
22 B. T. Heaton, L. Longhetti, D. M. P. Mingos, C. E. Briant, P. C. Minshall, B. R. C. Theobald, L. Garlaschelli and V. Sartorelli, *J. Organomet. Chem.*, 1981, **213**, 333.
23 G. Ciani, L. Garlaschelli, M. Manassero and U. Sartorelli, *J. Organomet. Chem.*, 1977, **129**, C25.
24 F. H. Carré, F. A. Cotton and B. A. Frenz, *Inorg. Chem.*, 1976, **15**, 380.
25 J. D. Jamerson, R. L. Pruett, E. Billing and F. A. Fiato, *J. Organomet. Chem.*, 1980, **193**, C43.
26 C. P. Lau, C. Y. Ren, L. Book and T. C. W. Mak, *J. Organomet. Chem.*, 1983, **249**, 429.
27 J. R. Kennedy, P. Selz, A. L. Rheingold, W. C. Trogler and F. Basolo, *J. Am. Chem. Soc.*, 1989, **111**, 3615.
28 S. J. Maginn, *Acta Crystallogr., Sect. C*, 1990, **46**, 576.
29 M. R. Churchill and J. P. Hutchinson, *Inorg. Chem.*, 1978, **17**, 5328.
30 D. Braga, R. Ros and R. Roulet, *J. Organomet. Chem.*, 1985, **286**, C8.
31 F. Demartin, M. Manassero, M. Sansoni, L. Garlaschelli, C. Raimondi, S. Martinengo and F. Canziani, *J. Chem. Soc., Chem. Commun.*, 1981, 528.
32 R. Bau, M. Y. Chiang, C.-Y. Wei, L. Garlaschelli, S. Martinengo and T. F. Koetzle, *Inorg. Chem.*, 1984, **23**, 4758.
33 G. Ciani, M. Manassero and A. Sironi, *J. Organomet. Chem.*, 1980, **199**, 271.
34 L. Garlaschelli, S. Martinengo, P. Chini, F. Canziani and R. Bau, *J. Organomet. Chem.*, 1981, **213**, 379.
35 J. N. Nicholls, P. R. Raithby and M. D. Vargas, *J. Chem. Soc., Chem. Commun.*, 1986, 1617.
36 R. Ros, A. Scrivanti, V. G. Albano, D. Braga and L. Garlaschelli, *J. Chem. Soc., Dalton Trans.*, 1986, 2411.
37 M. R. Churchill and J. P. Hutchinson, *Inorg. Chem.*, 1980, **19**, 2765.
38 D. Tranqui, A. Durif, M. Nasr Eddine, J. Lieto, J. J. Rafalko and B. C. Gates, *Acta Crystallogr., Sect. B*, 1982, **38**, 1916.
39 D. Braga, F. Grepioni, G. Guadalupi, A. Scrivanti, R. Ros and R. Roulet, *Organometallics*, 1987, **6**, 56.
40 V. G. Albano, D. Braga, F. Grepioni, R. Ros and A. Scrivanti, unpublished work.
41 D. J. Darensbourg and B. J. Baldwin-Zuschke, *Inorg. Chem.*, 1981, **20**, 3846.
42 M. M. Harding, B. S. Nicholls and A. K. Smith, *Acta Crystallogr., Sect. C*, 1984, **40**, 790.
43 V. G. Albano, D. Braga, R. Ros and A. Scrivanti, *J. Chem. Soc., Chem. Commun.*, 1985, 866.
44 A. J. Blake and A. G. Osborne, *J. Organomet. Chem.*, 1984, **260**, 227.
45 G. Ciani, M. Manassero, V. G. Albano, F. Canziani, G. Giordano, S. Martinengo and P. Chini, *J. Organomet. Chem.*, 1978, **150**, C17.
46 F. Demartin, M. Manassero, M. Sansoni, L. Garlaschelli and U. Sartorelli, *J. Organomet. Chem.*, 1981, **204**, C10.
47 U. Florke and H.-J. Haupt, *Z. Kristallogr.*, 1990, **191**, 149.
48 A. Strawczynski, R. Ros, R. Roulet, F. Grepioni and D. Braga, *Helv. Chim. Acta*, 1988, **71**, 1885.
49 F. Ragaini, F. Porta and F. Demartin, *Organometallics*, 1991, **10**, 185.
50 A. Strawczynski, R. Ros, R. Roulet, D. Braga, C. Gradella and F. Grepioni, *Inorg. Chim. Acta*, 1990, **170**, 17.

51 (*a*) R. Della Pergola, L. Garlaschelli, S. Martinengo, F. DeMartin, M. Manassero and M. Sansoni, *Gazz. Chim. Ital.*, 1987, **117**, 245; (*b*) M. P. Brown, D. Burns, M. M. Harding, S. Maginn and A. K. Smith, *Inorg. Chim. Acta*, 1989, **162**, 287.
52 J. A. Clucas, M. M. Harding, B. S. Nicholls and A. K. Smith, *J. Chem. Soc., Chem. Commun.*, 1984, 319.
53 M. R. Churchill and J. P. Hutchinson, *Inorg. Chem.*, 1979, **18**, 2451.
54 D. Braga and F. Grepioni, *J. Organomet. Chem.*, 1987, **336**, C9.
55 D. Braga and F. Grepioni, *J. Chem. Soc., Dalton Trans.*, 1993, 1223.
56 D. Braga, F. Grepioni, P. Sabatino and G. R. Desiraju, *Organometallics*, 1994, **13**, 3532; D. Braga, K. Biradha, F. Grepioni, V. R. Pedireddi and G. R. Desiraju, *J. Am. Chem. Soc.*, 1995, **117**, 3156.
57 D. Braga, F. Grepioni, P. Milne, E. Parisini, *J. Am. Chem. Soc.*, 1993, **115**, 5115.
58 P. Chini, *Inorg. Chim. Acta Rev.*, 1968, **2**, 31.
59 D. G. Evans and D. M. P. Mingos, *Organometallics*, 1983, **2**, 435; D. M. P. Mingos and D. J. Wales, *Introduction to Cluster Chemistry*, Prentice-Hall, Englewood Cliffs, NJ, 1990; R. G. Wooley, *Nouv. J. Chim.*, 1981, **5**, 441; K. C. C. Kharas and L. F. Dahl, *Adv. Chem. Phys.*, 1988, **70**, 1.
60 (*a*) J. W. Lauher, *J. Am. Chem. Soc.*, 1978, **100**, 5305; (*b*) C. Minot and M. Criado-Sancho, *Nouv. J. Chim.*, 1984, **8**, 537.
61 D. Braga, F. Grepioni, M. J. Calhorda and L. F. Veiros, *Organometallics*, 1995, **14**, 121.
62 D. L. Thorn and R. Hoffmann, *Inorg. Chem.*, 1978, **17**, 126; S. Shaik and R. Hoffmann, *J. Am. Chem. Soc.*, 1980, **102**, 1194; E. D. Jemmis, A. R. Pinhas and R. J. Hoffmann, *J. Am. Chem. Soc.*, 1980, **102**, 2576; D. G. Evans, *J. Chem. Soc., Chem. Commun.*, 1983, 675; R. H. Crabtree and M. Lavin, *Inorg. Chem.*, 1986, **25**, 805; A. A. Low, K. L. Kunze, P. J. MacDougall and M. B. Hall, *Inorg. Chem.*, 1991, **30**, 1079; A. Sironi, *Inorg. Chem.*, 1992, **31**, 2467.
63 D. Braga, F. Grepioni, E. Tedesco, M. J. Calhorda and P. E. M. Lopes, *J. Chem. Soc., Dalton Trans.*, following paper; D. Braga, F. Grepioni, H. Wadepohl, S. Gebert, M. J. Calhorda and L. F. Veiros, *Organometallics*, in the press.
64 D. Braga and F. Grepioni, in *Advances in Molecular Structure Research*, eds. I. Hargittai and M. Hargittai, JAI Press, Greenwich, in the press; V. G. Albano and D. Braga, in *Accurate Molecular Structures*, eds. A. Domenicano and I. Hargittai, Oxford University Press, Oxford, 1991.
65 A. I. Kitaigorodsky, *Solid State Sciences*, Springer, Berlin, 1984, vol. 33.
66 A. Gavezzotti, *J. Am. Chem. Soc.*, 1989, **111**, 1835.
67 A. I. Kitaigorodsky, *Molecular Crystals and Molecules*, Academic Press, New York, 1973.
68 D. Braga, J. J. Byrne, F. Grepioni and A. Wolf, *J. Chem. Soc., Chem. Commun.*, 1995, 1023.
69 J. H. Ammeter, H.-B. Bürgi, J. C. Thibeault and R. Hoffmann, *J. Am. Chem. Soc.*, 1978, **100**, 3686.
70 C. Mealli and D. M. Proserpio, *J. Chem. Educ.*, 1990, **67**, 39.
71 A. Gavezzotti, OPEC, Organic Packing Potential Energy Calculations, University of Milan, 1982; *J. Am. Chem. Soc.*, 1983, **195**, 5220.
72 A. L. Spek, PLATON, *Acta Crystallogr., Sect. A*, 1990, **46**, C31.
73 E. Keller, SCHAKAL 92, University of Freiburg, 1992.

Received 27*th February* 1995; *Paper* 5/01153A